JACS
JOURNAL OF THE AMERICAN CHEMICAL SOCIETY
pubs.acs.org/JACS
Communication

μMap-FFPE: A High-Resolution Protein Proximity Labeling Platform for Formalin-Fixed Paraffin-Embedded Tissue Samples

Noah B. Bissonnette, Marie E. Zamanis, Steve D. Knutson, Zane Boyer, Angelo Harris, Daniel Martin, Jacob B. Geri, Suzana Couto, Tahamtan Ahmadi, Anantharaman Muthuswamy, Mark Fereshteh, and David W. C. MacMillan*

Cite This: J. Am. Chem. Soc. 2025, 147, 23387−23394
Read Online

ABSTRACT: Many disease states can be understood by elucidating small-scale biomolecular protein interaction networks, or microenvironments. Photoproximity labeling methods, like μMap, have recently emerged as high-resolution techniques for mapping spatial relationships within subcellular architectures. However, *in vitro* models typically utilized lack the cell-type heterogeneity and three-dimensional structure essential for translating findings to clinical settings. To this end, formalin-fixed paraffin-embedded (FFPE) tissues are invaluable model systems for biomedical research, as they preserve complex multicellular interaction networks in their natural environment. While identifying microscale interactions in these samples could provide critical clinical insights, chemical modifications introduced during formalin-fixation and de-cross-linking are incompatible with standard photoproximity labeling techniques. Herein, we introduce μMap-FFPE, a new labeling system that enables comparison of the CD20 interactome across healthy cells, cancerous cells, and preserved patient tissues.

Biological interaction networks—comprising complex associations of proteins, nucleic acids, and metabolites—orchestrate cellular processes like signal transduction and gene expression. Dysregulation of these networks underlies disease phenotypes, making the elucidation of signaling pathways highly relevant for drug development.[1−4] Yet, mapping these *in vivo* connections is complicated, as protein−protein interactions can differ drastically between reductionist laboratory-based model systems—often homogeneous, immortalized cell lines—and patients in the clinic.[5−7] Typical cellular models fail to adequately capture key *in vivo* features of tissue, such as cell type heterogeneity and three dimensionality.[8] The ability to profile these attributes in clinical samples would greatly enhance personalized medicine and aid in the translation of potent cell-based therapeutics to approved drugs.[9] High-resolution interrogation of these protein interaction networks in primary patient tissue could also facilitate drug target validation and drive the development of precision therapeutics.[10]

Photocatalytic proximity labeling is an emerging technology capable of probing microscale interactions.[11,12] Many labeling platforms have been introduced, enabling the exploration of interactomes in a variety of biological contexts.[13] However, most methods are developed specifically for simple cellular model systems and often require genetic engineering to install the labeling ensemble,[14−17] precluding their use in tissue samples. Although some methods have been shown to be compatible with complex biological samples such as whole blood,[18] there is a dearth of *high-resolution techniques* applicable to human tissue. Recently, Fadeyi and co-workers disclosed a near-infrared proximity labeling system capable of tagging whole tissue using fluoroalkyl iodides and an organic photocatalyst.[19] Similar advancements demonstrated the tractability of tissue photolabeling with Ir or porphyrin-based catalysts,[20−22] yet these techniques utilize freshly harvested tissue samples for spatial proteomics. This feature significantly limits applications, as the most readily available forms of human tissue are formalin-fixed paraffin-embedded (FFPE) samples. Unlike fresh tissue, FFPE samples are stable for decades.[23] Estimates of worldwide FFPE samples range from 400 million to >1 billion, across thousands of diseases, representing a wealth of clinical information.[24,25] However, fixation fundamentally alters the molecular identity of the sample, greatly complicating sample preparation and analysis with traditional LC-MS/MS techniques, and the effect of fixation on photoproximity labeling mechanisms is poorly understood.[26] *Thus, we set out to develop a photoproximity labeling platform capable of generating spatial proteomic information within FFPE biological samples* (Figure 1). After establishing a labeling manifold for FFPE samples and studying its labeling mechanism, we examined the CD20 interactome, a B-cell marker and the target of multiple FDA-approved monoclonal antibodies,[27,28] in human tissue. We also compared CD20s interaction network across single cell type cultures and tissues, identifying fundamental differences in the interactomes between model systems. Finally, we validated novel CD20 proximal proteins identified by μMap-FFPE using super-resolution microscopy (STED).[29]

Received: April 16, 2025
Revised: June 2, 2025
Accepted: June 23, 2025
Published: June 26, 2025

https://doi.org/10.1021/jacs.5c06489
J. Am. Chem. Soc. 2025, 147, 23387−23394

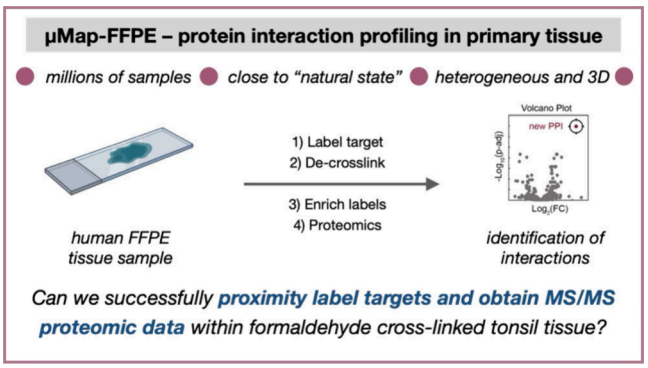

Figure 1. Development of μMap-FFPE.

We first attempted photolabeling FFPE cancer cells with μMap-Blue, which uses a 2° antibody-Ir catalyst conjugate to activate a diazirine probe upon blue-light irradiation.[11] Surprisingly, irrespective of labeling, washing, and epitope retrieval protocols, significant background labeling was observed by microscopy. Strikingly, when the Ir catalyst was omitted, we observed nonspecific, blue-light mediated photoactivation of the diazirine probe (**1**) (Figure 2a, conditions C). Diazirenes are not activated by blue-light wavelengths, as they only absorb UV-light. This implicates an endogenous photosensitizing capability of the FFPE sample, potentially arising from the fixation process itself. Indeed, similar results were obtained via Western blot in HEK293T cells after formalin-cross-linking (Figure S1). This suggests a formalin-induced formation of a blue-light photosensitizer, rendering μMap-Blue techniques incompatible with FFPE samples. Interestingly, this background activation was wavelength-dependent; it was not observed with our μMap-Red platform, which uses a conjugated Sn-chlorin catalyst and azide probe (**2**) (Figure 2a).[18] Using μMap-Red, we sought to identify the interactors of CD20 in FFPE human tonsils with proximity labeling using label-free proteomics. This requires mechanically harvesting, chemically de-cross-linking, and solubilizing the tissue,[30] then enriching the biotinylated proteins with streptavidin-coated beads. Many methods exist for reconstituting FFPE tissue: we sought to identify conditions that maximize recovery of free CD20 and total protein.[31] We tested several protocols and buffer solutions and found that 4% SDS, 80 mM HEPES, 80 mM DTT, pH 8 ("buffer B") was optimal, yielding minimized protein aggregation and better resolved protein migration via electrophoresis (Figure S2).[32] Furthermore, formalin-fixed cells that were de-cross-linked using these conditions gave identical band patterns to unfixed cells by Western blot (Figure S3), indicating reconstitution to a "native-like" state, a requirement for successful identification by MS-MS techniques.[26] However, when this protocol was applied to μMap-Red-labeled samples, significant biotinylation was observed by Western blot for all conditions where Bt-Az (**2**) was added (Figure 2b, lanes A-D). Given the contrast to our microscopy studies, we hypothesized that the conditions utilized for de-cross-linking (95 °C) promotes thermal activation of residual Bt-Az probe, forming a nitrene (**3**)[33,34] that labels proteins nonspecifically,[35,36] eliminating spatiotemporal information (Figure 2c). Unfortunately, attempts to wash away residual probe before de-cross-linking were unsuccessful. Recognizing the incompatibility of our photolabeling systems with FFPE samples, we sought to redesign μMap-Red to overcome these challenges. Typically μMap-Red functions by converting **2** to the active aminyl radical (**4**) via reduction by photogenerated Sn(III) followed by N_2 loss and protonation.[18] Cognizant of the key intermediacy of an aminyl radical, we questioned if this species could instead be generated by reductive quenching of the excited Sn^{IV} catalyst (Sn^{IV}*/Sn^{III} $E_{1/2}^{ox}$ = 1.25 V vs Ag/AgCl) with a biotin aniline conjugate, **5** (Bt-An, $E_{p/2}$ = 0.71 V vs Ag/AgCl). We speculated that a thermally stable aniline probe could avoid nonspecific labeling during heat-induced de-cross-linking (Figure 2c). We evaluated the relative thermal stability of Bt-Az (**2**) and Bt-An (**5**) under de-cross-linking conditions. Predictably, **5** showed minimal thermal activation whereas **2** displayed significant thermal labeling (Figure 2d). Furthermore, when the Sn/aniline system was utilized for proximity labeling of CD20 in FFPE human tonsil slides, labeling (after extraction) was only observed in the presence of the Sn photocatalyst. Thus, a thermally stable, photoproximity labeling system (μMap-FFPE) was successfully realized. Further optimization of conditions improved targeted labeling above background (lane A vs B) to ~2:1 (SI Section 14). Gratifyingly, μMap-FFP-labeled samples show strong biotinylation at germinal centers in tonsil (consistent with the localization of B-cells in tissue, Figure 2e).[37]

With a new probe in hand, we next evaluated the mechanism of activation and labeling (see Supporting Information (SI) for extended discussion). Pleasingly, Bt-An labeling was also under photonic control as labeling was seen only during short pulses of irradiation (2 min), implicating the catalytic relevance of Sn(IV)* (Figure 3a). However, *in vitro* labeling studies on bovine serum albumin (BSA) and carbonic anhydrase (CA) convoluted our mechanistic analysis. Presuming a redox mechanism is operative, a sacrificial oxidant, like oxygen, is required to turn over the photocatalyst. Interestingly, labeling *was* observed under N_2 for BSA, though *not* CA. This finding suggests an alternative pathway, wherein interchain disulfide bonds ($E_{1/2}^{red} \geq -0.71$ V vs SCE),[38] present in BSA but not CA, can serve as oxidants (Figure 3b). This hypothesis is supported by the restoration of CA labeling under anaerobic conditions when proteins with disulfide bonds are added (Figure S4), suggesting a redox labeling mechanism under N_2. However, our analysis for aerobic conditions is complicated by an additional, well-characterized proximity labeling mechanism.[14,15,39−42] This alternative pathway relies on sensitization of $^3O_2$ (**8**) by the excited state catalyst (**7**). Next, $^1O_2$ (**9**) covalently modifies nearby residues, such as histidine (**10**), via [4 + 2] cycloaddition and ring opening to furnish an electrophile (**11**). Upon nucleophilic attack by Bt-An covalently tagged **12** is generated.[43] Given the different residue modifications obtained by each labeling mechanisms (+Bt-An vs + Bt-An-O-H_2), we sought to implicate the primary pathway by detecting the adduct with DDA LC-MS/MS proteomics using open residue modification search. Interestingly, only mass shifts corresponding to the $^1O_2$ pathway were identified (+Bt-An-O-H_2), implicating O_2 sensitization as the dominant labeling pathway (Figure 3c). However, we cannot rule out a mixed redox/sensitization mechanism given the successful labeling of BSA under N_2. Thus, we propose that under air, $^1O_2$ is the primary reactive intermediate, while under N_2 the aminyl radical is responsible for labeling (Figure 3d).

With a better understanding of the μMap-FFPE platform, we performed LC-MS/MS proteomics on CD20 in human tonsil slides. Pleasingly, CD20 and other known interactors were highly enriched (Figure 4A),[44] including SRC kinases (LYN/FYN), which associate with B-cell surface receptors to enable signaling,[45] and many HLAs (DRA, DRB1/4).[46] Additionally,

https://doi.org/10.1021/jacs.5c06489
J. Am. Chem. Soc. 2025, 147, 23387−23394

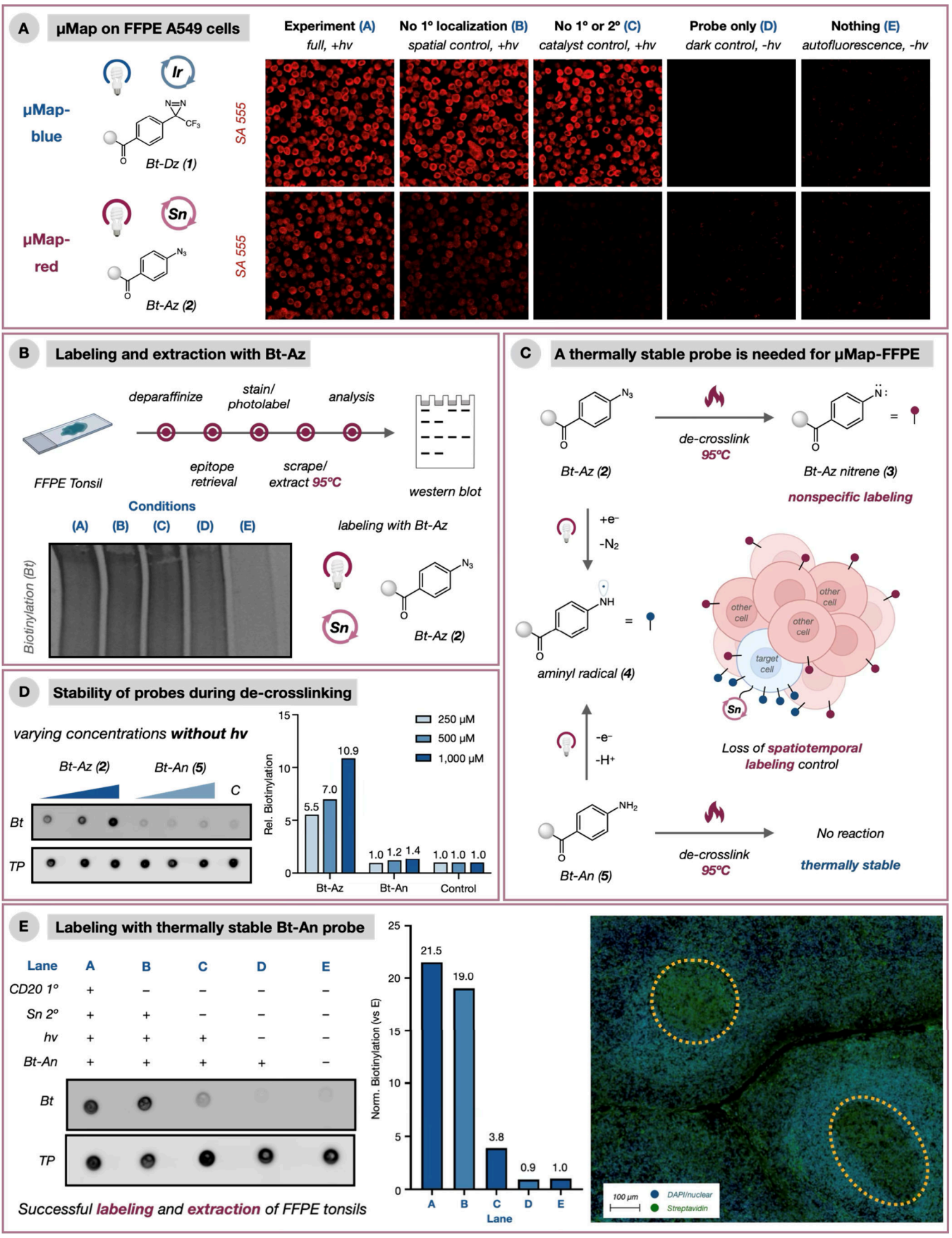

Figure 2. Incompatibility of μMap-Blue/Red with FFPE samples. (A) Photoproximity labeling of FFPE A549 cells (biotinylation in red). (B) μMap-Red with FFPE tonsil. (C) Thermal instability of Bt-Az causes nonspecific labeling. (D) Comparison of probe stability during de-cross-linking. (E) Successful CD20 labeling on FFPE tonsil, hv = 10 min. See SI for further optimization.

https://doi.org/10.1021/jacs.5c06489
J. Am. Chem. Soc. 2025, 147, 23387−23394

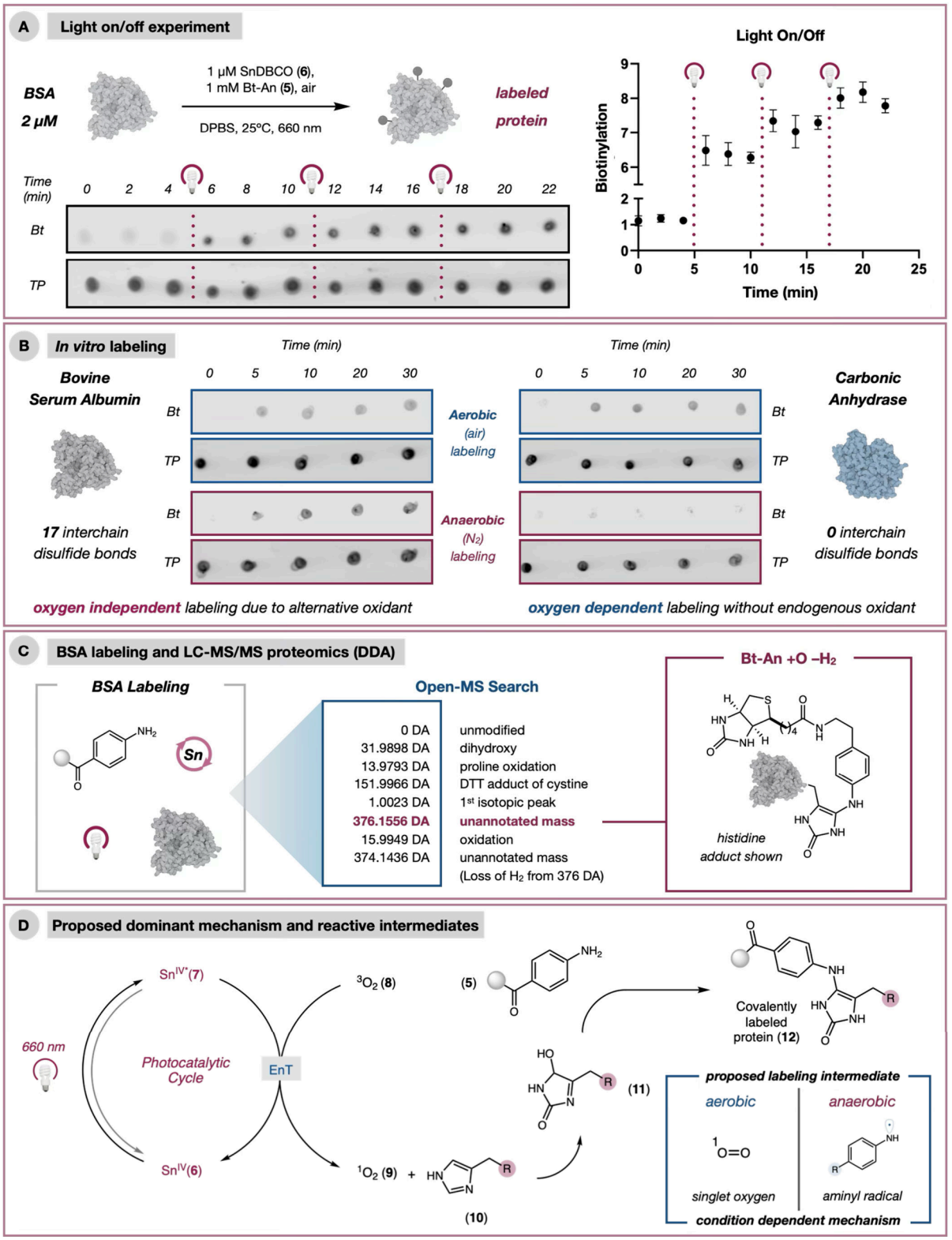

Figure 3. Mechanistic studies for μMap-FFPE. TP = total protein. DBCO = dibenzocyclooctyne. DPBS = Dulbecco's Phosphate-Buffered Saline. (A) Light on/off BSA labeling. Darkness for 6 min, then irradiation at 660 nm for 2 min. (B) *In vitro* labeling. (C) Detection of Bt-An-BSA labeling adduct under O_2 by LC-MS/MS DDA. (D) Proposed labeling mechanism and intermediates.

CD19, CD40, and CD79—known neighbors of CD20—were greatly enriched.[47,48] To benchmark our platform against established enzymatic proximity labeling methods, we targeted CD20 in tonsils with APEX labeling.[49,50] Gratifyingly, CD20 and several known interactors were enriched in both data sets. However, APEX captures only 14.3% of enriched proteins identified by μMap-FFPE, likely driven by altered labeling mechanisms and radii (SI Section 18).[51] To probe differences between μMap platforms, we performed μMap-Blue with human peripheral blood mononuclear cells (PBMCs) targeting

https://doi.org/10.1021/jacs.5c06489
J. Am. Chem. Soc. 2025, 147, 23387−23394

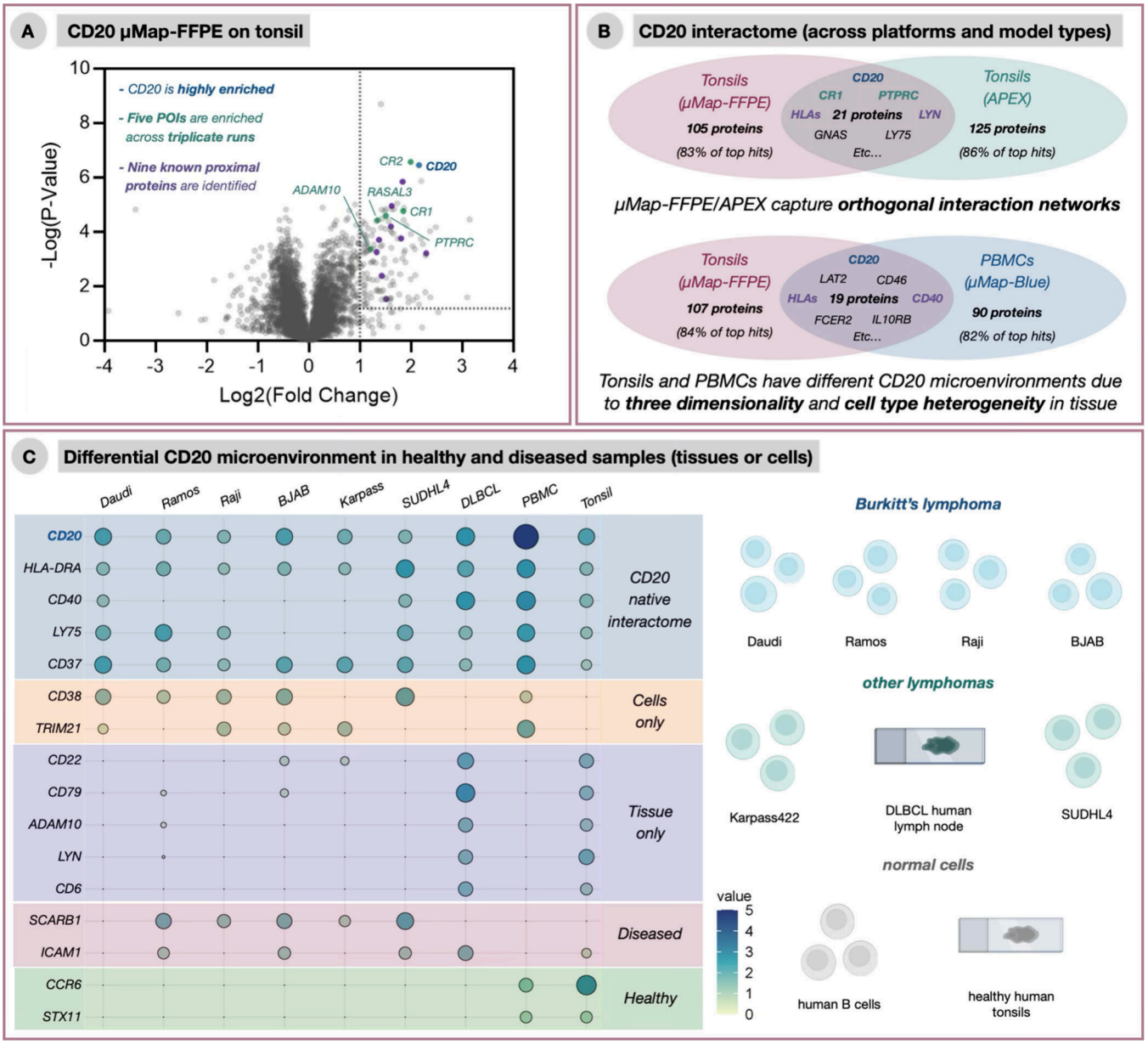

Figure 4. Photoproximity labeling of CD20. POI = Protein of interest. (A) μMap-FFPE on tonsils. (B) Comparison of CD20s interactome across techniques and models. (C) Balloon plot summarizing the interactome across models. See SI for all data sets.

CD20 (Figure 4B). Gratifyingly, CD20 and other top hits (CD40/MHCs) were enriched in both data sets. Despite this overlap, certain proteins that were highly enriched in tonsils were not observed in PBMCs, underscoring fundamental differences in B-cells between cells and tissue. These altered microenvironments are attributed to changes in model type, rather than labeling platform, as μMap-FFPE-labeled SUDHL4 cells (DLBCL line) and DLBCL tissue show a similarly low degree of overlap (Figure S5). We then conducted an extensive comparison between tissue and cells, as well as healthy and diseased model systems (using μMap-Blue/FFPE). Interestingly, CD20 and other neighbors were enriched across all data sets, supporting a common interactome. Yet, significant differences were also observed among model types. For example, CD38 and TRIM21 were uniquely enriched in cellular models, whereas CD22/79, ADAM10, LYN, and CD6 were only seen in tissues. Certain tissue-specific interactors can be explained by cell type heterogeneity, as CD6 is a common T-cell marker.[52] Furthermore, intracellular interactors (i.e., LYN), are identified in tissue as these samples have been permeabilized, enabling diffusion of the labeling intermediate across the membrane. Finally, disease-specific proximal proteins were found in DLCBL tissue and cancer cell lines, illustrating μMap's ability to discover interactions of potential pathological relevance (Figure 4C).

To validate novel proteins found in the tonsil CD20 microenvironment, we utilized STED microscopy. As a positive control, we examined the known interaction of CD20/IgD, which showed colocalization in tonsils (r = 0.669).[53] Across triplicate CD20 μMap-FFPE experiments in tonsils, 10 proteins were consistently enriched, including known interactors like HLAs. Yet, this data set also contained proteins that, to our knowledge, have not been identified within the CD20 microenvironment (ADAM10, CD21/45, and RASAL3).[47,48] Using STED, we validated the colocalization of all these proteins

https://doi.org/10.1021/jacs.5c06489
J. Am. Chem. Soc. 2025, 147, 23387−23394

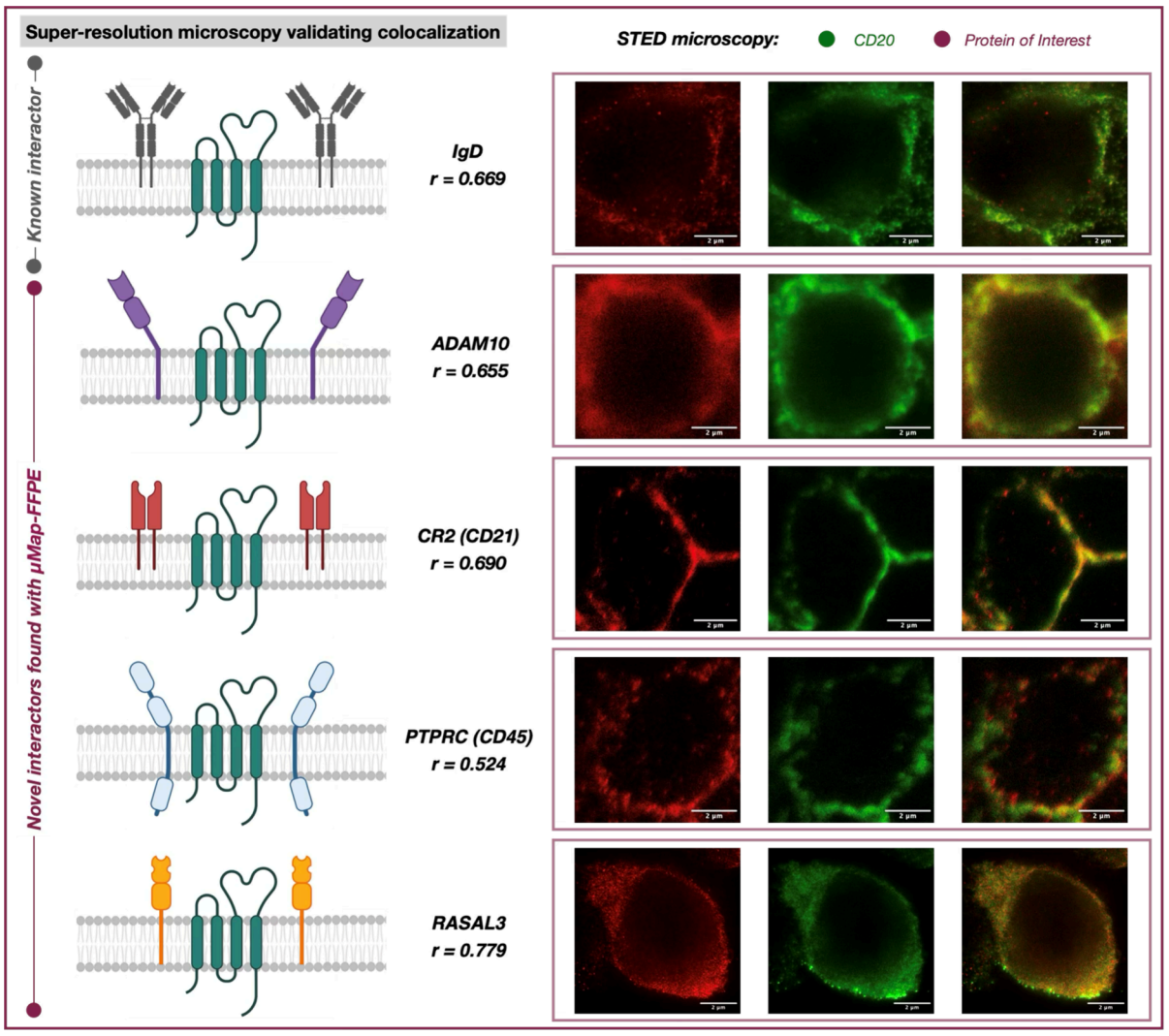

Figure 5. Validation of novel CD20 neighbors in FFPE tonsil using STED (r = Pearson's Coefficient).

with CD20 (r = 0.524−0.779),[54] establishing µMap-FFPE's ability to identify novel protein microenvironments in FFPE samples (Figure 5). These interactions were further validated by proximity ligation assay (PLA, Figure S6). The CD20/ADAM10 interaction is of interest, as ADAM10 is a metalloprotease that cleaves membrane-bound proteins, generating their soluble form. The loss of membrane-bound CD20, driven by a range of mechanisms,[55] is a well-characterized resistance pathway for treatments targeting CD20. Although further functional studies are required, understanding this interaction may suggest an orthogonal, ADAM10-mediated resistance pathway.

In conclusion, we have developed a photoproximity labeling technique, µMap-FFPE, compatible with the vast libraries of preserved tissue samples. Utilizing a red-light-activated catalytic manifold and thermally stable probe was key to the realization of this hypothesis-generating technology. Furthermore, we illustrated key differences between biological model systems, identifying differential interaction networks between types. Finally, new CD20 interactors were validated by STED/PLA. Collectively, µMap-FFPE is a new tool within the field of proximity labeling, situated to prosecute protein interactions in FFPE samples across biological contexts and disease states.

■ ASSOCIATED CONTENT

Supporting Information

The Supporting Information is available free of charge at https://pubs.acs.org/doi/10.1021/jacs.5c06489.

Proteomics Data for BSA Labeling (XLSX)

Additional experimental details, protocols, and characterization data (PDF)

Combined Raw Proteomics Data − CD20 Labeling (XLSX)

■ AUTHOR INFORMATION

Corresponding Author

David W. C. MacMillan − *Merck Center for Catalysis at Princeton University, Princeton, New Jersey 08544, United States;* orcid.org/0000-0001-6447-0587; Email: dmacmill@princeton.edu

Authors

Noah B. Bissonnette − *Merck Center for Catalysis at Princeton University, Princeton, New Jersey 08544, United States;* orcid.org/0000-0001-6892-5040

Marie E. Zamanis − *Genmab US, Inc., Princeton, New Jersey 08540, United States*

Steve D. Knutson − *Merck Center for Catalysis at Princeton University, Princeton, New Jersey 08544, United States*
Zane Boyer − *Merck Center for Catalysis at Princeton University, Princeton, New Jersey 08544, United States;* orcid.org/0009-0002-3739-9134
Angelo Harris − *Genmab US, Inc., Princeton, New Jersey 08540, United States*
Daniel Martin − *Genmab US, Inc., Princeton, New Jersey 08540, United States*
Jacob B. Geri − *Merck Center for Catalysis at Princeton University, Princeton, New Jersey 08544, United States;* orcid.org/0000-0002-9215-5610
Suzana Couto − *Genmab US, Inc., Princeton, New Jersey 08540, United States*
Tahamtan Ahmadi − *Genmab US, Inc., Princeton, New Jersey 08540, United States*
Anantharaman Muthuswamy − *Genmab US, Inc., Princeton, New Jersey 08540, United States*
Mark Fereshteh − *Genmab US, Inc., Princeton, New Jersey 08540, United States*

Complete contact information is available at: https://pubs.acs.org/10.1021/jacs.5c06489

Notes

The authors declare the following competing financial interest(s): D.W.C.M. declares a competing financial interest with respect to the integrated photoreactor. Additionally, D.W.C.M. declares an ownership interest in the company Dexterity Pharma LLC, which has commercialized materials used in this work.

■ ACKNOWLEDGMENTS

Research reported in this work was supported by the National Institute of General Medical Sciences of the National Institutes of Health (R35GM134897), the Ludwig Institute for Cancer Research, the Princeton Catalysis Initiative, and Genmab. N.B.B. and Z.B. thank the Taylor family for the Edward C. Taylor Fellowship. S.D.K. acknowledges the NIH for post-doctoral fellowships (1F32GM142206 and 1K99GM154140). The authors thank Brandon J. Bloomer and Sean W. Huth for helpful scientific discussions and Rebecca Lambert for assistance in preparing the manuscript.

■ ABBREVIATIONS

FFPE, formalin-fixed paraffin-embedded; Bt-Dz, biotin diazerane; Bt-Az, biotin azide; Bt-An, biotin aniline; BSA, bovine serum albumin; CA, carbonic anhydrase; DDA, data-dependent acquisition; DBCO, dibenzocyclooctyne; DPBS, Dulbecco's Phosphate-Buffered Saline; POI, protein of interest; PMBCs, Peripheral Blood Mononuclear Cells; DLBCL, diffuse large B-cell lymphoma; STED, stimulated emission depletion

■ REFERENCES

(1) De Las Rivas, J.; Fontanillo, C. Protein−Protein Interaction Networks: Unraveling the Wiring of Molecular Machines within the Cell. *Brief Funct Genomics* **2012**, *11*, 489−496.
(2) Lu, H.; Zhou, Q.; He, J.; Jiang, Z.; Peng, C.; Tong, R.; Shi, J. Recent Advances in the Development of Protein−Protein Interactions Modulators: Mechanisms and Clinical Trials. *Signal Transduct. Target. Ther.* **2020**, *5*, 213.
(3) Shin, W. H.; Kumazawa, K.; Imai, K.; Hirokawa, T.; Kihara, D. Current Challenges and Opportunities in Designing Protein−Protein Interaction Targeted Drugs. *Adv. Appl. Bioninform. Chem.* **2020**, *13*, 11−25.
(4) Greenblatt, J. F.; Alberts, B. M.; Krogan, N. J. Discovery and Significance of Protein-Protein Interactions in Health and Disease. *Cell* **2024**, *187*, 6501−6517.
(5) Bledsoe, M. J.; Grizzle, W. E. The Use of Human Tissues for Research: What Investigators Need to Know. *Altern. Lab Anim.* **2022**, *50*, 265−274.
(6) Seok, J.; Warren, H. S.; Alex, G. C.; Michael, N. M.; Henry, V. B.; Xu, W.; Richards, D. R.; McDonald-Smith, G. P.; Gao, H.; Hennessy, L.; Finnerty, C. C.; López, C. M.; Honari, S.; Moore, E. E.; Minei, J. P.; Cuschieri, J.; Bankey, P. E.; Johnson, J. L.; Sperry, J.; Nathens, A. B.; Billiar, T. R.; West, M. A.; Jeschke, M. G.; Klein, M. B.; Gamelli, R. L.; Gibran, N. S.; Brownstein, B. H.; Miller-Graziano, C.; Calvano, S. E.; Mason, P. H.; Cobb, J. P.; Rahme, L. G.; Lowry, S. F.; Maier, R. V.; Moldawer, L. L.; Herndon, D. N.; Davis, R. W.; Xiao, W.; Tompkins, R. G. Genomic Responses in Mouse Models Poorly Mimic Human Inflammatory Diseases. *Proc. Natl. Acad. Sci. U. S. A.* **2013**, *110*, 3507−3512.
(7) Vargas-Rondón, N.; Pérez-Mora, E.; Villegas, V. E.; Rondón-Lagos, M. Role of Chromosomal Instability and Clonal Heterogeneity in the Therapy Response of Breast Cancer Cell Lines. *Cancer Biol. Med.* **2020**, *17*, 970−985.
(8) Altschuler, S. J.; Wu, L. F. Cellular Heterogeneity: When Do Differences Make a Difference? *Cell* **2010**, *141*, 559−563.
(9) Sun, D.; Gao, W.; Hu, H.; Zhou, S. Why 90% of Clinical Drug Development Fails and How to Improve It? *Acta Pharm. Sin B* **2022**, *12*, 3049−3062.
(10) Akbarzadeh, S.; Coşkun, Ö.; Günçer, B. Studying Protein−Protein Interactions: Latest and Most Popular Approaches. *J. Struct Biol.* **2024**, *216*, No. 108118.
(11) Geri, J. B.; Oakley, J. V.; Reyes-Robles, T.; Wang, T.; McCarver, S. J.; White, C. H.; Rodriguez-Rivera, F. P.; Parker, D. L.; Hett, E. C.; Fadeyi, O. O.; Oslund, R. C.; MacMillan, D. W. C. Microenvironment Mapping via Dexter Energy Transfer on Immune Cells. *Science* **2020**, *367*, 1091−1097.
(12) Knutson, S. D.; Buksh, B. F.; Huth, S. W.; Morgan, D. C.; MacMillan, D. W. C. Current Advances in Photocatalytic Proximity Labeling. *Cell Chem. Biol.* **2024**, *31*, 1145−1161.
(13) Fang, Y.; Zou, P. Photocatalytic Proximity Labeling for Profiling the Subcellular Organization of Biomolecules. *ChemBioChem.* **2023**, *24*, No. e202200745.
(14) Hananya, N.; Ye, X.; Koren, S.; Muir, T. W. A Genetically Encoded Photoproximity Labeling Approach for Mapping Protein Territories. *Proc. Natl. Acad. Sci. U. S. A.* **2023**, *120*, No. e2219339120.
(15) Zheng, F.; Zhou, X.; Zou, P.; Yu, C. Genetically Encoded Photocatalytic Protein Labeling Enables Spatially-Resolved Profiling of Intracellular Proteome. *Nat. Commun.* **2023**, *14*, 2978.
(16) Pan, C.; Knutson, S. D.; Huth, S. W.; MacMillan, D. W. C. μMap Proximity Labeling in Living Cells Reveals Stress Granule Disassembly Mechanisms. *Nat. Chem. Biol.* **2025**, *21*, 490.
(17) Knutson, S. D.; Pan, C. R.; Bisballe, N.; Bloomer, B. J.; Raftopolous, P.; Saridakis, I.; MacMillan, D. W. C. Parallel Proteomic and Transcriptomic Microenvironment Mapping (μMap) of Nuclear Condensates in Living Cells. *J. Am. Chem. Soc.* **2025**, *147*, 488−497.
(18) Buksh, B. F.; Knutson, S. D.; Oakley, J. V.; Bissonnette, N. B.; Oblinsky, D. G.; Schwoerer, M. P.; Seath, C. P.; Geri, J. B.; Rodriguez-Rivera, F. P.; Parker, D. L.; Scholes, G. D.; Ploss, A.; Macmillan, D. W. C. μMap-Red: Proximity Labeling by Red Light Photocatalysis. *J. Am. Chem. Soc.* **2022**, *144*, 6154−6162.
(19) Ryu, K. A.; Reyes-Robles, T.; Wyche, T. P.; Bechtel, T. J.; Bertoch, J. M.; Zhuang, J.; May, C.; Scandore, C.; Dephoure, N.; Wilhelm, S.; Quasem, I.; Yau, A.; Ingale, S.; Szendrey, A.; Duich, M.; Oslund, R. C.; Fadeyi, O. O. Near-Infrared Photoredox Catalyzed Fluoroalkylation Strategy for Protein Labeling in Complex Tissue Environments. *ACS Catal.* **2024**, *14*, 3482−3491.
(20) Liu, Z.; Guo, F.; Zhu, Y.; Qin, S.; Hou, Y.; Guo, H.; Lin, F.; Chen, P. R.; Fan, X. Bioorthogonal Photocatalytic Proximity Labeling in Primary Living Samples. *Nat. Commun.* **2024**, *15*, 2712.

(21) Lou, Z.; Zhang, Y.; Liang, X.; Cao, M.; Ma, Y.; Chen, P. R.; Fan, X. Deep-Red and Ultrafast Photocatalytic Proximity Labeling Empowered In Situ Dissection of Tumor-Immune Interactions in Primary Tissues. *J. Am. Chem. Soc.* **2025**, *147*, 9716−9726.
(22) Tong, F.; Zhou, W.; Janiszewska, M.; Seath, C. P. Multiprobe Photoproximity Labeling of the EGFR Interactome in Glioblastoma Using Red-Light. *J. Am. Chem. Soc.* **2025**, *147*, 9316−9327.
(23) Koh, J. M. S.; Sykes, E. K.; Rukhaya, J.; Anees, A.; Zhong, Q.; Jackson, C.; Panizza, B. J.; Reddel, R. R.; Balleine, R. L.; Hains, P. G.; Robinson, P. J. The Effect of Storage Time and Temperature on the Proteomic Analysis of FFPE Tissue Sections. *Clin Proteomics* **2025**, *22*, 5.
(24) Sah, S.; Chen, L.; Houghton, J.; Kemppainen, J.; Marko, A. C.; Zeigler, R.; Latham, G. J. Functional DNA Quantification Guides Accurate Next-Generation Sequencing Mutation Detection in Formalin-Fixed, Paraffin-Embedded Tumor Biopsies. *Genome Med.* **2013**, *5*, 77.
(25) Blow, N. Tissue Issues. *Nature* **2007**, *448*, 959−960.
(26) Nirmalan, N. J.; Harnden, P.; Selby, P. J.; Banks, R. E. Mining the Archival Formalin-Fixed Paraffin-Embedded Tissue Proteome: Opportunities and Challenges. *Mol. BioSyst.* **2008**, *4*, 712−720.
(27) Casan, J. M. L.; Wong, J.; Northcott, M. J.; Opat, S. Anti-CD20 Monoclonal Antibodies: Reviewing a Revolution. *Hum. Vaccin. Immunother.* **2018**, *14*, 2820−2841.
(28) Dabkowska, A.; Domka, K.; Firczuk, M. Advancements in Cancer Immunotherapies Targeting CD20: From Pioneering Monoclonal Antibodies to Chimeric Antigen Receptor-Modified T Cells. *Front. Immunol.* **2024**, *15*, No. 1363102.
(29) Bückers, J.; Kastrup, L.; Wildanger, D.; Vicidomini, G.; Hell, S. W. Simultaneous Multi-Lifetime Multi-Color STED Imaging for Colocalization Analyses. *Opt. Express* **2011**, *19*, 3130−3143.
(30) Magdeldin, S.; Yamamoto, T. Toward Deciphering Proteomes of Formalin-Fixed Paraffin-Embedded (FFPE) Tissues. *Proteomics* **2012**, *12*, 1045−1058.
(31) García-Vence, M.; Chantada-Vazquez, M.; del, P.; Sosa-Fajardo, A.; Agra, R.; Barcia de la Iglesia, A.; Otero-Glez, A.; García-González, M.; Cameselle-Teijeiro, J. M.; Nuñez, C.; Bravo, J. J.; Bravo, S. B. Protein Extraction From FFPE Kidney Tissue Samples: A Review of the Literature and Characterization of Techniques. *Front. Med.* **2021**, *8*, No. 657313.
(32) Kawashima, Y.; Kodera, Y.; Singh, A.; Matsumoto, M.; Matsumoto, H. Efficient Extraction of Proteins from Formalin-Fixed Paraffin-Embedded Tissues Requires Higher Concentration of Tris-(Hydroxymethyl)Aminomethane. *Clin. Proteom.* **2014**, *11*, 4.
(33) Boyer, J. H.; Canter, F. C. Alkyl and Aryl Azides. *Chem. Rev.* **1954**, *54*, 1−57.
(34) Smolinsky, G. Thermal Reactions of Substituted Aryl Azides : The Nature of the Azene Intermediate. *J. Am. Chem. Soc.* **1961**, *83*, 2489−2493.
(35) Tay, N. E. S.; Ryu, K. A.; Weber, J. L.; Olow, A. K.; Cabanero, D. C.; Reichman, D. R.; Oslund, R. C.; Fadeyi, O. O.; Rovis, T. Targeted Activation in Localized Protein Environments via Deep Red Photoredox Catalysis. *Nat. Chem.* **2023**, *15*, 101−109.
(36) Zhang, Y.; Tan, J.; Chen, Y. Visible-Light-Induced Protein Labeling in Live Cells with Aryl Azides. *Chem. Commun.* **2023**, *59*, 2413−2420.
(37) Victora, G. D.; Nussenzweig, M. C. Germinal Centers. *Annu. Rev. Immunol.* **2022**, *40*, 413−442.
(38) Cook, K. M. Determining the Redox Potential of a Protein Disulphide Bond. In *Functional Disulphide Bonds*; Hogg, P., Ed.; Humana: New York, 2019; pp 65−86.
(39) Nakane, K.; Sato, S.; Niwa, T.; Tsushima, M.; Tomoshige, S.; Taguchi, H.; Ishikawa, M.; Nakamura, H. Proximity Histidine Labeling by Umpolung Strategy Using Singlet Oxygen. *J. Am. Chem. Soc.* **2021**, *143*, 7726−7731.
(40) Qiu, S.; Li, W.; Deng, T.; Bi, A.; Yang, Y.; Jiang, X.; Li, J. P. Ru(Bpy)32+-Enabled Cell-Surface Photocatalytic Proximity Labeling toward More Efficient Capture of Physically Interacting Cells. *Angew. Chem., Int. Ed.* **2023**, *62*, No. e202303014.
(41) Miura, K.; Niimi, H.; Niwa, T.; Taguchi, H.; Nakamura, H. Intracellular Photocatalytic Proximity Labeling (IPPL) for Dynamic Analysis of Chromatin-Binding Proteins Targeting Histone H3. *ACS Chem. Biol.* **2024**, *19*, 2412−2417.
(42) Nakane, K.; Nagasawa, H.; Fujimura, C.; Koyanagi, E.; Tomoshige, S.; Ishikawa, M.; Sato, S. Switching of Photocatalytic Tyrosine/Histidine Labeling and Application to Photocatalytic Proximity Labeling. *Int. J. Mol. Sci.* **2022**, *23*, 11622.
(43) Matsukawa, R.; Yamane, M.; Kanai, M. Histidine Photooxygenation Chemistry: Mechanistic Evidence and Elucidation. *Chem. Rec.* **2023**, *23*, No. e202300198.
(44) Pavlasova, G.; Mraz, M. The Regulation and Function of CD20: An "Enigma" of B-Cell Biology and Targeted Therapy. *Haematologica* **2020**, *105*, 1494−1506.
(45) Deans, J. P.; Kalt, L.; Ledbetter, J. A.; Schieven, G. L.; Bolen, J. B.; Johnson, P. Association of 75/80-KDa Phosphoproteins and the Tyrosine Kinases Lyn, Fyn, and Lck with the B Cell Molecule CD20: Evidence against Involvement of the Cytoplasmic Regions of CD20. *J. Biol. Chem.* **1995**, *270*, 22632−22638.
(46) Wilkinson, S. T.; Vanpatten, K. A.; Fernandez, D. R.; Brunhoeber, P.; Garsha, K. E.; Glinsmann-Gibson, B. J.; Grogan, T. M.; Teruya-Feldstein, J.; Rimsza, L. M. Partial Plasma Cell Differentiation as a Mechanism of Lost Major Histocompatibility Complex Class II Expression in Diffuse Large B-Cell Lymphoma. *Blood* **2012**, *119*, 1459−1467.
(47) Szklarczyk, D.; Kirsch, R.; Koutrouli, M.; Nastou, K.; Mehryary, F.; Hachilif, R.; Gable, A. L.; Fang, T.; Doncheva, N. T.; Pyysalo, S.; Bork, P.; Jensen, L. J.; Von Mering, C. The STRING Database in 2023: Protein−Protein Association Networks and Functional Enrichment Analyses for Any Sequenced Genome of Interest. *Nucleic Acids Res.* **2023**, *51*, D638−D646.
(48) Oughtred, R.; Rust, J.; Chang, C.; Breitkreutz, B. J.; Stark, C.; Willems, A.; Boucher, L.; Leung, G.; Kolas, N.; Zhang, F.; Dolma, S.; Coulombe-Huntington, J.; Chatr-aryamontri, A.; Dolinski, K.; Tyers, M. The BioGRID Database: A Comprehensive Biomedical Resource of Curated Protein, Genetic, and Chemical Interactions. *Protein Sci.* **2021**, *30*, 187−200.
(49) Rhee, H. W.; Zou, P.; Udeshi, N. D.; Martell, J. D.; Mootha, V. K.; Carr, S. A.; Ting, A. Y. Proteomic Mapping of Mitochondria in Living Cells via Spatially Restricted Enzymatic Tagging. *Science* **2013**, *339*, 1328−1331.
(50) Killinger, B. A.; Marshall, L. L.; Chatterjee, D.; Chu, Y.; Bras, J.; Guerreiro, R.; Kordower, J. H. In Situ Proximity Labeling Identifies Lewy Pathology Molecular Interactions in the Human Brain. *Proc. Natl. Acad. Sci. U. S. A.* **2022**, *119*, No. e2114405119.
(51) Oakley, J. V.; Buksh, B. F.; Fernández, D. F.; Oblinsky, D. G.; Seath, C. P.; Geri, J. B.; Scholes, G. D.; MacMillan, D. W. C. Radius Measurement via Super-Resolution Microscopy Enables the Development of a Variable Radii Proximity Labeling Platform. *Proc. Natl. Acad. Sci. U. S. A.* **2022**, *119*, No. e2203027119.
(52) Gonçalves, C. M.; Henriques, S. N.; Santos, R. F.; Carmo, A. M. CD6, a Rheostat-Type Signalosome That Tunes T Cell Activation. *Front. Immunol.* **2018**, *9*, 2994.
(53) Kläsener, K.; Jellusova, J.; Andrieux, G.; Salzer, U.; Böhler, C.; Steiner, S. N.; Albinus, J. B.; Cavallari, M.; Süß, B.; Voll, R. E.; Boerries, M.; Wollscheid, B.; Reth, M. CD20 as a Gatekeeper of the Resting State of Human B Cells. *Proc. Natl. Acad. Sci. U. S. A.* **2021**, *118*, No. e2021342118.
(54) Bolte, S.; Cordelières, F. P. A Guided Tour into Subcellular Colocalization Analysis in Light Microscopy. *J. Microsc* **2006**, *224*, 213−232.
(55) Schuster, S. J.; Huw, L. Y.; Bolen, C. R.; Maximov, V.; Polson, A. G.; Hatzi, K.; Lasater, E. A.; Assouline, S. E.; Bartlett, N. L.; Budde, L. E.; Matasar, M. J.; Koeppen, H.; Piccione, E. C.; Wilson, D.; Wei, M. C.; Yin, S.; Penuel, E. Loss of CD20 Expression as a Mechanism of Resistance to Mosunetuzumab in Relapsed/Refractory B-Cell Lymphomas. *Blood* **2024**, *143*, 822−832.

https://doi.org/10.1021/jacs.5c06489
J. Am. Chem. Soc. 2025, 147, 23387−23394